AIAA JOURNAL
Vol. 42, No. 12, December 2004

Free Vibration Analysis of Rotating Blades with Uniform Tapers

Gang Wang* and Norman M. Wereley†
University of Maryland, College Park, Maryland 20742

A spectral finite element method (SFEM) is proposed to develop a low-degree-of-freedom model for dynamic analysis of rotating tapered beams. The method exploits semi-analytical progressive wave solutions of the governing partial differential equations. Only one single spectral finite element is needed to obtain any modal frequency or mode shape, which is as accurate or better than other approaches reported in the literature for straight or uniformly tapered beams. The minimum number of such spectral finite elements corresponds to the number of substructures, that is, beam sections with different uniform tapers, in a rotating beam to capture the complete system dynamic characteristics. The element assembly procedure is accomplished in the same fashion as the conventional finite element approach. Results are for a number of examples such as a straight beam and beams with uniform taper or compound tapers. Overall, for a rotating blade system, our SFEM provides highly accurate predictions for any modal frequency using a single element or very few elements corresponding to the number of uniform taper changes in the blade system.

Nomenclature

$EI(x)$	=	beam bending flexural stiffness
EI_0	=	reference beam bending flexural stiffness
L	=	beam length
$M(x)$	=	beam bending moment
$m(x)$	=	beam mass per unit length
m_0	=	reference beam mass per unit length
R	=	offset length between beam and rotating hub
$T(x)$	=	beam axial force due to centrifugal stiffening
$V(x)$	=	beam shear force
$W(x)$	=	beam bending mode shape function
$w(x, t)$	=	beam transverse displacement
α	=	beam mass per unit length constant
β_i	=	beam bending flexural stiffness constant, $i = 1, 4$
η	=	nondimensional axial force
μ	=	nondimensional natural frequency
Ω	=	beam rotation speed
ω	=	excitation frequency

Introduction

THE determination of modal frequencies and mode shape functions of rotating structural elements, such as helicopter blades, airplane propellers, windmill rotors, and other turbomachinery blades, is very important. There are many discussions available in the literature.[1–15] Leissa,[1] in his review paper, limited his scope to the studies of vibration of rotating blades. For a relatively long blade, the simplest representation of dynamic response is the Euler–Bernoulli beam model. A helicopter blade can undergo torsional motion, out-of-plane bending vibration (flapping), and in-plane vibration (lead–lag). In this study, we assume that there is no coupling among these motions, so that the transverse bending vibration can be studied independently. However, the blades do not need to have uniform cross-sectional area. We allow taper changes in a blade, and both mass and flexural stiffness distributions along a blade are represented as polynomial functions, which is typical in engineering applications.

Because of the centrifugal stiffening effect, the analysis of free vibration of rotating beams becomes a challenge. We can apply the classical Galerkin and assumed Ritz methods to the transverse vibration of rotating beams with tapers (see Ref. 16). However, we must choose the admissible (trial) functions that satisfy at least geometry boundary conditions in the Ritz method, or both geometry and natural boundary conditions in the Galerkin method. For different configurations of rotating beam systems, different admissible functions must be chosen, which is not convenient. Also, we must include many admissible functions to obtain sufficiently accurate modal frequency predictions for a rotating tapered beam, especially for higher modes, which leads to a large size eigenvalue problem. Conventional finite element methods (CFEM) can be easily modified to meet the changing of boundary conditions. Hodges and Rutkowski[2] developed a Ritz-displacement finite element model with variable order to analyze rotating uniform and tapered beams, where the shape functions were assumed to be Legendre polynomial functions. Also, they reviewed previous efforts to calculate the natural frequencies of rotating beams. Some typical approaches used to solve natural frequencies of rotating beams were discussed, including the Southwell principle (see Ref. 3), the integrating matrix method,[4] the Rayleigh–Ritz method (see Ref. 5), the perturbation method,[6,7] and the Galerkin finite element (see Ref. 8). Other finite element-based approaches were given by Murty and Murthy,[9] Dzygadlo and Sobieraj,[10] Putter and Manor,[11] Hoa,[12] Hodges,[13] Khulief,[14] and Udupa and Varadan.[15] Those finite element models can be extended to tapered beam cases. Because the modal frequency predictions in these finite element models converge as the number of elements increases, we must include many elements in the finite element model to achieve accuracy of natural frequency predictions even for lower modes, which leads to a large size eigenvalue problem. To apply the resulting large-degree-of-freedom finite element method (FEM) model in a dynamic simulation (forced or transient), or to embed such a model in a real-time model-based control problem, can be impractical. As a result, the model order must be reduced via static or dynamic condensation procedures to a practical number of degrees of freedom, which is constrained by simulation time, or the control interval in a digital control system. Therefore, we need an approach that has a substantially reduced order of degrees of freedom compared to CFEM but maintains high accuracy of mode frequency, mode shape, and force response predictions for rotating beams.

Spectral FEM (also called dynamic stiffness method) is a candidate to provide such high accuracy using fewer number of elements. Doyle[17] developed the spectral finite element models for the problem of longitudinal vibration of rods and transverse bending vibration

Received 1 August 2003; revision received 9 July 2004; accepted for publication 20 July 2004.

*Assistant Research Scientist, Smart Structures Laboratory, Department of Aerospace Engineering, Alfred Gessow Rotorcraft Center; gwang@glue.umd.edu. Member AIAA.

†Professor, Smart Structures Laboratory, Department of Aerospace Engineering, Alfred Gessow Rotorcraft Center; wereley@eng.umd.edu. Associate Fellow AIAA.

of nonrotating uniform Euler–Bernoulli beams. Leung[18] also discussed the dynamics stiffness method in the structural dynamic analyses. Because the spectral FEM or dynamic stiffness method was developed in the frequency domain, the natural frequencies were determined by solving transcendental equations instead of eigenvalue problems as in the conventional finite element model. The corresponding mode shapes were then determined at each natural frequency. In the spectral finite element model, the shape functions were duplicated from exact wave propagation solutions from the governing equation. Therefore, one single element can capture any modal frequency and mode shape. For the structural force or transient response calculations, a fast Fourier transform (FFT)/inverse FFT transformation technique must be used between the time domain and the frequency domain. We have successfully applied the spectral finite element methodology to the analysis of sandwich beams with viscoelastic damping materials.[19] A substantially reduced number of elements, compared to CFEM, were needed to achieve comparable or better accuracy of natural frequency and response predictions for sandwich beams. Also, because the mode shape functions were given in a semi-analytical form based on the progressive wave solution from the governing equation, the mode shape results can be documented for future similar applications. Basically, we can establish a mode shape database for tapered rotating beams instead of recalculating the mode shape functions in the future.

To develop a spectral finite element model for tapered rotating beams, we must obtain the analytical structure of the solutions first. Because of the tapers and centrifugal stiffening effects, it is difficult to solve the problem analytically. However, for uniform or simple tapered rotating beams, we still can obtain semi-analytical solutions. Usually, the power series or Frobenius method (extended power series) method can be used to solve the ordinary differential equations with nonconstant coefficients (see Refs. 20 and 21). Giurgiutiu and Stafford[22] solved the vibration of uniform rotating beam using power series approach. Wright et al.[23] applied the Frobenius method and solved the natural frequencies for both uniform and tapered rotating beams with cantilever or hinged boundary conditions, in which the tapered beam has linear variations of mass and flexural stiffness along beam span. The natural frequency results of uniform beams were compared to those obtained by Hodges and Rutkowski,[2] where a variable-order Ritz displacement FEM was used. Harris[24] presented an analytical test case for rotor flapping bending responses, in which power series solution was used to define the deflection and the corresponding forcing function was solved backward to satisfy the fourth-order flapping governing equations. Recently, Naguleswaran[25] also studied the lateral vibration of a centrifugally tensioned uniform Euler–Bernoulli beam using the Frobenius method. Naguleswaran provided many frequency results for uniform rotating beams with different boundary conditions and investigated the effect of offset between beam and rotating hub. Banerjee[26] proposed a dynamic stiffness method based on the Frobenius solutions of a uniform rotating beam. The dynamic stiffness method was applied to uniform and tapered rotating beams. For a uniform rotating beam, one single element was needed to capture the whole dynamic characteristics of bending vibration. A tapered beam was approximated by 20–50 uniform beam elements, where the results of natural frequency yielded comparable accuracy as those obtained by Hodges and Rutkowski[2] and Wright et al.[23] Huang and Liu[27] proposed a dynamic stiffness method for a rotating beam of nonuniform cross section. The cross-sectional area was assumed to have a general polynomial form and power series were used to obtain exact solution of the governing equations. The research focused on how to calculate time response. The mass and stiffness matrices were reconstructed using the dynamic stiffness matrix in the frequency domain. They did not exploit the modal frequency and modal shape calculations for the rotating beams, which is very important for rotor dynamic analysis.

In this paper, we will extend the spectral FEM to analyze bending vibrations of a type of tapered beam under rotation. We assume that mass variation along the beam span is linear and stiffness distribution is a polynomial function with up to fourth order. Those assumptions are valid for most practical helicopter blades.[28] Based on the Frobenius method (extended power series method), we develop semi-analytical solutions for tapered beams under rotation. Then we apply spectral finite element techniques to solve for the unknown wave coefficients using nodal degrees of freedom. This leads to a standard matrix representation of dynamic characteristics for a rotating tapered beam element. The natural frequencies can be determined using boundary conditions in the free vibration case. Cantilever or hinged boundary conditions were considered in this paper to represent boundary conditions for hingeless or articulated rotor blades. Examples investigated both by Hodges and Rutkowski[2] and Wright et al.[23] are used to validate our natural frequency predictions based on our tapered spectral finite element model. Also our predictions of natural frequency of tapered beams are compared to the results by Banerjee,[26] where the dynamic stiffness matrix method was used to analyze a tapered rotating beam based on the uniform spectral finite element. Both uniform and tapered beams were investigated at different rotating speeds and with either cantilevered or hinged boundary conditions. The results are as good or better than those reported in the cited studies, but in our model only one single spectral finite element was used. Mode shape functions were calculated as well. A helicopter blade with compound taper was also used to validate our spectral finite element model, which was studied by Hodges.[13] There were two taper changes in the blade system. Therefore, only two spectral finite elements are needed to calculate the modal frequency results, where there were five elements needed to achieve convergent modal frequency prediction for the fourth mode in Hodges's analysis. Basically a rotating blade system, our spectral FEM provides highly accurate predictions for any modal frequency using a single element or very few elements corresponding to the number of uniform taper changes in the blade system. Also we obtain exact rotating mode shape functions, which can be used in future similar studies. In the following sections, we will present the details of our spectral finite element model for tapered blades under rotation.

Governing Equation of Rotating Beams

As shown in Fig. 1, a tapered beam element under rotation was presented. We now state the governing equations for beam out-of-plane bending vibration. As discussed by Wright et al.[23] and Banerjee,[26] the governing equation of free vibration for a rotating Euler–Bernoulli beam is

$$\frac{\partial^2}{\partial x^2}\left[EI(x)\frac{\partial^2 w}{\partial x^2}\right] - \frac{\partial}{\partial x}\left[T(x)\frac{\partial w}{\partial x}\right] + m(x)\frac{\partial^2 w}{\partial t^2} = 0 \qquad (1)$$

Governing equation (1) is expressed in terms of transverse displacement $w(x, t)$. $T(x)$ is the axial force due to the centrifugal stiffening:

$$T(x) = \int_x^L [m(x)\Omega^2(R + x)]\,dx + F \qquad (2)$$

Equation (2) is given by Hodges and Rutkowski.[2] F is an axial force applied at the end of beam element, as shown in Fig. 1. We assumed that variation of mass along beam length L was defined as

$$m(x) = m_0[1 + \alpha(x/L)] \qquad (3)$$

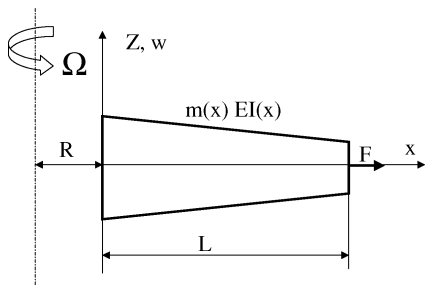

Fig. 1 Out-of-plane bending vibration of a tapered beam under rotation.

where m_0 is the mass per unit length at $x=0$ (reference mass), α is a taper parameter, and $\alpha \neq -1$, which results in singularity when $x=L$. Flexural stiffness variation along length of beam element was

$$EI(x) = EI_0\left[1+\beta_1(x/L)+\beta_2(x^2/L^2)+\beta_3(x^3/L^3)+\beta_4(x^4/L^4)\right] \tag{4}$$

where EI_0 is the flexural stiffness at $x=0$. Here $\beta_i, i=1,4$, are taper parameters for stiffness distribution. These parameters can be determined by α for beams with a rectangular cross-sectional area and thickness varying along the beam length. However, as with the example studied by Wright et al.,[23] the taper parameters for mass and flexural stiffness were not necessarily related. They are independent variables. However, these parameters cannot result in a singularity for flexural stiffness when $x=L$.

Substituting Eq. (3) into Eq. (2), we can integrate to find the axial force within a rotating beam element:

$$T(x) = \tfrac{1}{2}m_0\Omega^2(L^2+2RL-2Rx-x^2) + \tfrac{1}{6}m_0\Omega^2(\alpha/L)(2L^3+3RL^2-2Rx^2-2x^3)+F \tag{5}$$

The bending moment in the beam element is defined as

$$M(x) = EI(x)\frac{\partial^2 w}{\partial x^2} \tag{6}$$

and shear force is given by

$$V(x) = -\frac{\partial M}{\partial x} + T(x)\frac{\partial w}{\partial x} \tag{7}$$

When $T(x)=0$, Eq. (7) yields the same shear force expression as a classical nonrotating Euler–Bernoulli beam.

Spectral Finite Element Model

The governing equation of free vibration of a rotating tapered beam was presented in Eq. (1) The next step is to determine the solution via wave propagation method. Therefore, we assume that transverse displacement $w(x,t)$ under harmonic excitation is

$$w(x,t) = W(x)e^{j\omega t} \tag{8}$$

where ω is the excitation angular frequency. Substituting Eq. (8) into the governing Equation (1), yields the ordinary differential equation

$$EI(x)\frac{d^4W}{dx^4} + 2\frac{d}{dx}[EI(x)]\frac{d^3W}{dx^3} + \frac{d^2}{dx^2}[EI(x)]\frac{d^2W}{dx^2} - T(x)\frac{d^2W}{dx^2} - \frac{dT}{dx}\frac{dW}{dx} - m\omega^2 W = 0 \tag{9}$$

To present Eq. (9) in a nondimensional form, we define

$$X = \frac{x}{L}, \qquad \bar{W} = \frac{W}{L}, \qquad \frac{d}{dx} = \frac{1}{L}\frac{d}{dX}$$

The governing equation can be expressed in nondimensional form as

$$\left(1+\beta_1 X+\beta_2 X^2+\beta_3 X^3+\beta_4 X^4\right)\frac{d^4\bar{W}}{dX^4} + 2\left(\beta_1+2\beta_2 X+3\beta_3 X^2+4\beta_4 X^3\right)\frac{d^3\bar{W}}{dX^3} + \left(2\beta_2+6\beta_3 X+12\beta_4 X^2\right)\frac{d^2\bar{W}}{dX^2} - \left\{\lambda^2\left[\frac{1}{2}(1+2\bar{R}-2\bar{R}X-X^2) + \frac{1}{6}\alpha(3\bar{R}-3\bar{R}X^2+2-2X^3)\right]+\eta\right\}\frac{d^2\bar{W}}{dX^2} - \lambda^2[\bar{R}+X+\alpha(\bar{R}X+X^2)]\frac{d\bar{W}}{dX} - \mu^2(1+\alpha X)\bar{W} = 0 \tag{10}$$

where

$$\bar{R} = \frac{R}{L}, \qquad \lambda^2 = \frac{m_0\Omega^2L^4}{EI_0}, \qquad \eta = \frac{FL^2}{EI_0}, \qquad \mu^2 = \frac{m_0\omega^2L^4}{EI_0}$$

The nondimensional axial force $\bar{T}(X)$, bending moment $\bar{M}(X)$, and shear force $\bar{V}(X)$ are defined as

$$\bar{T}(X) = \frac{T(x)L^2}{EI_0} = \lambda^2\left[\frac{1}{2}(1+2\bar{R}-2\bar{R}X-X^2) + \frac{1}{6}\alpha(3\bar{R}-3\bar{R}X+2-2X^3)\right]+\eta$$

$$\bar{M}(X) = \frac{M(x)L}{EI_0} = \left(1+\beta_1 X+\beta_2 X^2+\beta_3 X^3+\beta_4 X^4\right)\frac{d^2\bar{W}}{dX^2}$$

$$\bar{V}(X) = \frac{V(x)L^2}{EI_0} = -\left(1+\beta_1 X+\beta_2 X^2+\beta_3 X^3+\beta_4 X^4\right)\frac{d^3\bar{W}}{dX^3} - \left(\beta_1+2\beta_2 X+3\beta_3 X^2+4\beta_4 X^3\right)\frac{d^2\bar{W}}{dX^2} + \bar{T}(X)\frac{d\bar{W}}{dX} \tag{11}$$

Equation (10) is a linear ordinary differential equation (ODE) with variable coefficients. This type of ODE can be solved using power series or Frobenius methods as discussed in Refs. 20 and 21. We adopted the Frobenius method and assume that the displacement function $\bar{W}(X)$ is

$$\bar{W}(X) = \sum_0^\infty a_n X^{n+c} \tag{12}$$

where a_n is the coefficient of the nth polynomial function and c can be determined later using an indicial equation. The derivatives of function $\bar{W}(X)$ are given by

$$\frac{d\bar{W}}{dX} = \sum_{n=0}^{\infty}(n+c)a_n X^{n+c-1}$$

$$\frac{d^2\bar{W}}{dX^2} = \sum_{n=0}^{\infty}(n+c)(n+c-1)a_n X^{n+c-2}$$

$$\frac{d^3\bar{W}}{dX^3} = \sum_{n=0}^{\infty}(n+c)(n+c-1)(n+c-2)a_n X^{n+c-3}$$

$$\frac{d^4\bar{W}}{dX^4} = \sum_{n=0}^{\infty}(n+c)(n+c-1)(n+c-2)(n+c-3)a_n X^{n+c-4} \tag{13}$$

Substituting Eqs. (12) and (13) into Eq. (10), we first obtain the following indicial equation[25]:

$$c(c-1)(c-2)(c-3) = 0 \tag{14}$$

Therefore, we have four roots for c, which are $c_i = 0, 1, 2, 3$, $i=1,4$. Based on these four roots, four linear independent solution functions for displacement $\bar{W}$ are obtained, as shown in Eq. (12). For each root of c, the coefficients of $a_n(c)$ can be determined using recurrence relationship by collecting same-order polynomial functions when substituting Eqs. (12) and (13) into

the governing equation (10). The results for the coefficients of $a_n(c)$ are

$$a_0(c) = 1$$

$$a_1(c) = -\frac{\beta_1(c-1)}{(c+1)}a_0(c)$$

$$a_2(c) = -\frac{\beta_1 c}{c+2}a_1(c) + \frac{\lambda^2\left[\frac{1}{2} + \bar{R} + \alpha\left(\frac{1}{2}\bar{R} + \frac{1}{3}\right)\right] + \eta}{(c+2)(c+1)}a_0(c) - \frac{\beta_2(c-1)}{c+2}a_0(c)$$

$$a_3(c) = -\frac{\beta_1(c+1)}{c+3}a_2(c) - \frac{\beta_2(c+1)c}{(c+3)(c+2)}a_1(c) + \frac{\lambda^2\left[\frac{1}{2} + \bar{R} + \alpha\left(\frac{1}{2}\bar{R} + \frac{1}{3}\right)\right] + \eta}{(c+3)(c+2)}a_1(c) - \frac{\beta_3(c+1)(c-1)c + \lambda^2\bar{R}c}{(c+3)(c+2)(c+1)}a_0(c)$$

$$a_4(c) = -\frac{\beta_1(c+2)}{c+4}a_3(c) - \frac{\beta_2(c+2)(c+1)}{(c+4)(c+3)}a_2(c) + \frac{\lambda^2\left[\frac{1}{2} + \bar{R} + \alpha\left(\frac{1}{2}\bar{R} + \frac{1}{3}\right)\right] + \eta}{(c+4)(c+3)}a_2(c) - \frac{\beta_3(c+2)(c+1)c + \lambda^2\bar{R}(c+1)}{(c+4)(c+3)(c+2)}a_1(c) - \frac{\beta_4(c-1)c}{(c+4)(c+3)}a_0(c) - \frac{\lambda^2\left[\frac{1}{2} + (\alpha/2)\bar{R}\right](c+1)c - \mu^2}{(c+4)(c+3)(c+2)(c+1)}a_0(c)$$

$$a_{n+5}(c) = -\frac{\beta_1(n+c+3)}{n+c+5}a_{n+4}(c) - \frac{\beta_2[(n+c+1)(n+c+4)+2]}{(n+c+5)(n+c+4)}a_{n+3}(c) + \frac{\lambda^2\left[\frac{1}{2} + \bar{R} + \alpha\left(\frac{1}{2}\bar{R} + \frac{1}{3}\right)\right] + \eta}{(n+c+5)(n+c+4)}a_{n+3}(c) - \frac{\beta_3(n+c+1)[(n+c)(n+c+5)+6]}{(n+c+5)(n+c+4)(n+c+3)}a_{n+2}(c) - \frac{\lambda^2\bar{R}(n+c+2)}{(n+c+5)(n+c+4)(n+c+2)}a_{n+2}(c) - \frac{\beta_4(n+c+1)(n+c)[(n+c-1)(n+c+6)+12]}{(n+c+5)(n+c+4)(n+c+3)}a_{n+1}(c) - \frac{\lambda^2\left[\frac{1}{2} + (\alpha/2)\bar{R}\right](n+c+1)(n+c) - \mu^2}{(n+c+5)(n+c+4)(n+c+3)(n+c+2)}a_{n+1}(c) - \frac{(\lambda^2/3)\alpha(n+c)(n+c+2) - \mu^2\alpha}{(n+c+5)(n+c+4)(n+c+3)(n+c+2)}a_n(c)$$

$$n = 0, 1, \ldots, \infty \quad (15)$$

Then we can construct our solution for the displacement function $\bar{W}$:

$$\bar{W}(X) = A_1F_1(X) + A_2F_2(X) + A_3F_3(X) + A_4F_4(X) \quad (16)$$

where the unknown wave amplitudes A_i, $i = 1, 2, 3, 4$, can be determined from boundary conditions. The four linearly independent polynomial functions $F_i(X)$, $i = 1, 2, 3, 4$, are defined by

$$F_i(X) = \sum_{n=0}^{\infty} a_n(c_i)X^{n+c_i} \quad (17)$$

where the coefficients $a_n(c_i)$ were determined using Eq. (15) for corresponding roots of c.

Now we have obtained an exact solution as shown in Eq. (16). The natural frequencies and mode shapes can be determined by applying the boundary conditions and solving a transcendental equation to obtain a nontrivial solution for the four wave amplitudes A_1, A_2, A_3, and A_4. This process has been applied to bending vibration of nonrotating uniform Euler–Bernoulli beam (see Ref. 29). However, to present a standard matrix representation and capture the dynamic characteristics for a rotating beam element, we introduce the spectral finite element method,[17,18] where we borrow the concept of nodal degrees of freedom from the conventional finite element model. First, these nodal degrees of freedom are used to solve unknown wave amplitudes A_i, $i = 1, 4$. Second, we calculate the corresponding nodal forces and introduce the stiffness matrix, which is the relationship between the nodal forces and nodal degrees of freedom. Because the interpolation functions in the spectral finite element were duplicated from the exact wave propagation solution instead of using polynomial functions as in the conventional finite element model, one single element can be used to compute any modal frequency and corresponding mode shape. For the bending vibration of a nonrotating uniform Euler–Bernoulli beam, Doyle[18] has presented the details. We have applied the same methodology to the sandwich beam analysis.[19] Banerjee[26] also applied it to bending vibration of uniform rotating beams and developed the dynamic stiffness matrix. For a tapered beam, Banerjee discretized it using many uniform elements to achieve acceptable accuracy for the natural frequency calculations. Therefore, we extend the spectral FEM to tapered rotating beams. Using our method, a single tapered spectral finite element can be used to analyze either uniform or nonuniform (tapered) beams under rotation. Because we have obtained exact solutions of the tapered rotating beam, the remaining derivation is straightforward. Figure 2 shows the taper spectral finite element for a rotating beam. Similar to the classical beam bending finite element, the degrees of freedom are the displacements and slopes at each beam end. The corresponding nodal forces are transverse shear force and bending moment. The nodal degrees of freedom can be expressed by wave amplitudes:

$$\boldsymbol{q} = [P]A \quad (18)$$

where $\boldsymbol{q}$ is nodal degrees of freedom vector, A contains four wave amplitudes, and P is a 4×4 matrix defining the relationship between these two vectors. They are

$$\boldsymbol{q} = [\bar{W}_1 \quad \bar{W}_1' \quad \bar{W}_2 \quad \bar{W}_2']^T$$

$$A = [A_1 \quad A_2 \quad A_3 \quad A_4]^T$$

$$P = \begin{bmatrix} 1 & 0 & 0 & 0 \\ F_1'(0) & 1 & 0 & 0 \\ F_1(1) & F_2(1) & F_3(1) & F_4(1) \\ F_1'(1) & F_2'(1) & F_3'(1) & F_4'(1) \end{bmatrix} \quad (19)$$

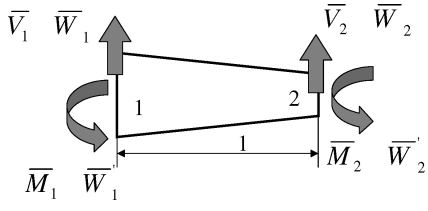

Fig. 2 Spectral finite element of a tapered beam under rotation.

When Eq. (11) is recalled, the bending moment and shear force can be determined by unknown wave amplitudes:

$$\begin{aligned}\bar{V}(X) &= -\left(1+\beta_1 X+\beta_2 X^2+\beta_3 X^3+\beta_4 X^4\right)\\ &\quad\times\left(A_1F_1'''+A_2F_2'''+A_3F_3'''+A_4F_4'''\right)\\ &\quad-\left(\beta_1+2\beta_2 X+3\beta_3 X^2+4\beta_4 X^3\right)\\ &\quad\times\left(A_1F_1''+A_2F_2''+A_3F_3''+A_4F_4''\right)\\ &\quad+\bar{T}(X)\left(A_1F_1'+A_2F_2'+A_3F_3'+A_4F_4'\right)\\ \bar{M}(X) &= \left(1+\beta_1 X+\beta_2 X^2+\beta_3 X^3+\beta_4 X^4\right)\\ &\quad\times\left(A_1F_1''+A_2F_2''+A_3F_3''+A_4F_4''\right)\end{aligned}\tag{20}$$

Now the nodal forces, as shown in Fig. 2, can be determined. When $X=0$,

$$\bar{V}(0)=-\bar{V}_1,\qquad \bar{M}(0)=-\bar{M}_1$$

When $X=1$,

$$\bar{V}(1)=\bar{V}_2,\qquad \bar{M}(1)=\bar{M}_2$$

Note that change in sign of nodal forces at each node, which is very important to obtain the correct stiffness matrix. Finally, the nodal force vectors $\boldsymbol{Q}$, which contain $\bar{V}_1$, $\bar{M}_1$, $\bar{V}_2$, and $\bar{M}_2$, are expressed by unknown wave amplitude vector $\boldsymbol{A}$:

$$\boldsymbol{Q}=[B]_{4\times 4}\boldsymbol{A}\tag{21}$$

where B matrix is a 4×4 matrix and each row is defined as

$$\begin{aligned}\boldsymbol{Q} &= [\bar{V}_1\quad \bar{M}_1\quad \bar{V}_2\quad \bar{M}_2]^T\\ B_{1i} &= F_i'''(0)+\beta_1F_i''(0)-\bar{T}(0)F_i'\\ B_{2i} &= -F_i''(0)\\ B_{3i} &= -(1+\beta_1+\beta_2+\beta_3+\beta_4)F_i'''(1)\\ &\quad-(\beta_1+2\beta_2+3\beta_3+4\beta_4)F_i''(1)+\bar{T}(1)F_i'(1)\\ B_{4i} &= (1+\beta_1+\beta_2+\beta_3+\beta_4)F_i''(1)\end{aligned}$$

Now the nodal force vector $\boldsymbol{Q}$ can be expressed by the vector of nodal degrees of freedom $\boldsymbol{q}$, which yields the spectral finite element stiffness matrix $\bar{k}$, which is a 4×4 symmetric matrix,

$$\bar{k}=BP^{-1}\tag{22}$$

Because the dynamic stiffness matrix $\bar{k}$ was derived and presented in a nondimensional form, we must present a dimensional form to assemble elements if there is more than one element used in the spectral finite element model. This process is straightforward and was also discussed by Banerjee.[26] Finally, our dynamic stiffness matrix is given by

$$\begin{bmatrix}V_1\\M_1\\V_2\\M_2\end{bmatrix}=\begin{bmatrix}k_{11}&k_{12}&k_{13}&k_{14}\\k_{12}&k_{22}&k_{23}&k_{24}\\k_{13}&k_{23}&k_{33}&k_{34}\\k_{14}&k_{24}&k_{34}&k_{44}\end{bmatrix}\begin{bmatrix}W_1\\W_1'\\W_2\\W_2'\end{bmatrix}\tag{23}$$

where the nodal force vector and nodal degrees of freedom vector are in dimensional form, the resulting stiffness matrix k can be determined by nondimensional stiffness matrix $\bar{k}$, as shown in Eq. (22) The elements in the stiffness matrix k are

$$\begin{aligned}k_{11} &= \left(EI_0/L^3\right)\bar{k}_{11},\qquad k_{12}=\left(EI_0/L^2\right)\bar{k}_{12}\\ k_{13} &= \left(EI_0/L^3\right)\bar{k}_{13},\qquad k_{14}=\left(EI_0/L^2\right)\bar{k}_{14}\\ k_{22} &= (EI_0/L)\bar{k}_{22},\qquad k_{23}=\left(EI_0/L^2\right)\bar{k}_{23}\\ k_{24} &= (EI_0/L)\bar{k}_{24},\qquad k_{33}=\left(EI_0/L^3\right)\bar{k}_{33}\\ k_{34} &= \left(EI_0/L^2\right)\bar{k}_{34},\qquad k_{44}=(EI_0/L)\bar{k}_{44}\end{aligned}\tag{24}$$

For free vibration analysis of rotating tapered beams, we must apply the boundary conditions to determine the natural frequencies and mode shapes. In the spectral finite element model, we will solve a transcendental equation instead of eigenvalue problem in the conventional finite element. Because only hingeless or articulated rotor blades were considered in this study, the corresponding boundary condition are cantilevered or hinged, respectively. For a hingeless rotor blade, the boundary conditions are

$$\begin{aligned}x=0,&\qquad W_1=0,&&\qquad W_1'=0\\ x=L,&\qquad V_2=0,&&\qquad M_2=0\end{aligned}\tag{25}$$

For example, there is only one element in the spectral finite element model. Substituting the preceding boundary conditions into the stiffness matrix, we obtain

$$\begin{bmatrix}k_{33}&k_{34}\\k_{34}&k_{44}\end{bmatrix}\begin{bmatrix}W_2\\W_2'\end{bmatrix}=0\tag{26}$$

For an articulated rotor blade, the boundary conditions are

$$\begin{aligned}x=0,&\qquad W_1=0,&&\qquad M_1=0\\ x=L,&\qquad V_2=0,&&\qquad M_2=0\end{aligned}\tag{27}$$

Similarly, substituting these boundary conditions into the stiffness matrix, we obtain the characteristic equation for a hinged beam,

$$\begin{bmatrix}k_{22}&k_{23}&k_{24}\\k_{23}&k_{33}&k_{34}\\k_{24}&k_{34}&k_{44}\end{bmatrix}\begin{bmatrix}W_1'\\W_2\\W_2'\end{bmatrix}=0\tag{28}$$

If we need more than one element to model the beam system, we first need to assemble the elements to obtain a total stiffness matrix. Then applying the boundary conditions, we should obtain similar forms as shown in Eqs. (26) and (28). However, it will not be same size as shown in Eqs. (26) and (28). The nontrivial solutions of Eq. (26) or (28) will yield the beam natural frequency, and the mode shape function can be calculated based on the corresponding natural frequency. Therefore, the determinant of the matrix as shown in Eq. (26) or (28) must be equal to zero. Because these matrices were developed in the frequency domain and are functions of unknown natural frequency ω, then the values of ω that cause the determinant to vanish yield the natural frequencies of the rotating beam. Therefore, we need to solve a transcendental equation in the spectral finite element model. In our calculations, we first give an initial guess of the modal frequency of interest. Figure 3 shows the determinant as a function of unknown frequency ω, for a cantilevered uniform beam with rotation speed $\lambda=1$. Because there are infinite solutions to vanish the determinant, we can calculate any natural frequency and mode shape as we wish. Then an iteration scheme is used to vanish the determinant of the characteristic equation in the spectral finite element model. The computation time for each iteration is fairly negligible, which is less than 1 s using MATLAB® subroutines. This procedure is different from the eigenvalue problem in the finite element model for the modal frequency predictions. For any known natural frequency, the corresponding mode shape function can be easily determined. These modal frequency and mode shape function are exact solutions of the governing equations. For the force responses, we only need to replace the right-hand terms in Eqs. (26) and (28) by applied external forces. Because the solutions for the Frobenius series have infinite terms, we must truncate the series for numerical simulations. However, the number of terms used was chosen for convergent $F_i(X)$, yielding similar frequency predictions compared to other results. Banerjee[26] suggested that 80

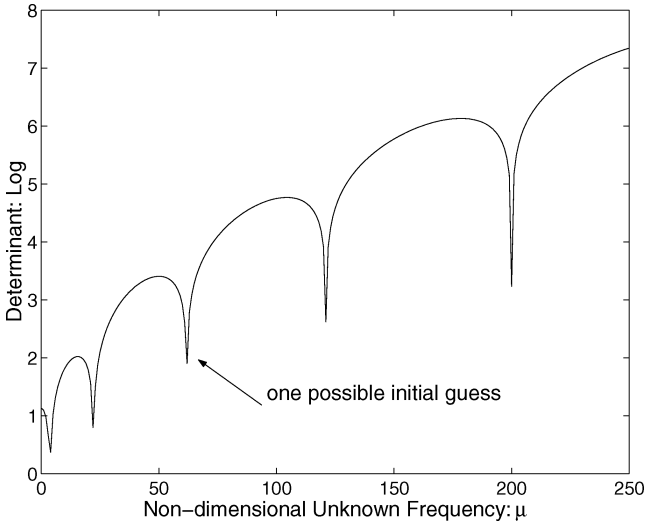

Fig. 3 Determinant of characteristic equation as a function of unknown frequency.

terms in the power series yields six digit accuracy and 120 terms can increase accuracy up to nine digits for uniform rotating beam natural frequency predictions. The number of terms included in the power series in this study was determined by achieving at least the same accuracy for natural frequency predictions based on the results from the literature. For the uniform beam, we included 50 terms in the Frobenius functions and 80 terms and 350 terms for uniform taper beams 1 and 2, respectively. For a helicopter blade with compound taper, we included 200 terms in the Frobenious series.

Uniform Beam Analysis

In this section, we validate our spectral finite element model using free vibration results of rotating beams. Uniform beams were considered. Cantilevered and hinged boundary conditions were assumed because those boundary conditions corresponding to hingeless and articulated rotor blades. Our analyses were analytically validated using the results in the literature. Wright et al.[23] developed the exact solutions for tapered beams using the Frobenius method, in which both flexural stiffness $EI(x)$ and mass unit length $m(x)$ varied linearly along the beam length. Hodges and Rutkowski[2] developed a variable-order Ritz displacement CFEM, in which the displacement shape functions were assumed by shift Legendre polynomial functions with order from 3 to 15. This variable-order FEM was developed to achieve desirable accuracy of the frequency predictions for rotating beams by either varying the order of interpolation functions or including more elements but with reduced order of polynomial functions used in the shape functions of finite element model. The results of using 1 element with 15-order polynomial shape functions were assumed to be the exact solution in their analyses.

Tables 1 and 2 show the natural frequency results for uniform rotating beams under cantilevered and hinged boundary conditions, respectively. The hub off set length $\bar{R}$ was assumed zero in both cases. In Table 1, the first five natural frequencies of a uniform rotating beam under cantilevred boundary conditions are presented, in which we considered two rotating speeds, $\lambda = 0$ and 12. Only one single spectral finite element was used to obtain these natural frequencies. Fifty terms ($n = 50$) were included in the Frobenius functions to match the accuracy of six digits of the solutions by Wright et al.[23] and Hodges and Rutkowski.[2] However, Hodges and Rutkowski[2] only presented the first three natural frequencies. All three analyses were matched well for the natural frequency prediction for the uniform cantilevered beam under rotation.

In Table 2, we present the natural frequency results for a uniform beam with hinged boundary conditions. Again, one single spectral finite element was used in our analysis and the first 50 terms were included in the Frobenius functions. The final results were validated against Wright et al.[23] results. We achieved six digits of accuracy in the natural frequency predictions.

Table 1 Prediction of nondimensional natural frequencies of cantilevered uniform beam

Mode	SFEM exact	Wright et al.[23] exact	Hodges and Rutkowski[2] CFEM
		$\lambda = 0$	
1	3.5160	3.5160	3.5160
2	22.0345	22.0345	22.0345
3	61.6972	61.6972	61.6972
4	120.902	120.902	N/A
5	199.860	199.860	N/A
		$\lambda = 12$	
1	13.1702	13.1702	13.1702
2	37.6031	37.6031	37.6031
3	79.6145	79.6145	79.6145
4	140.534	140.534	N/A
5	220.536	220.536	N/A

Table 2 Predictions of nondimensional natural frequencies of hinged uniform beam

Mode	SFEM exact	Ref. 23 exact
	$\lambda = 0$	
1	0.0	0.0
2	15.4182	15.4182
3	49.9649	49.9649
4	104.248	104.248
5	178.270	178.270
	$\lambda = 12$	
1	12.0000	12.0000
2	33.7603	33.7603
3	70.8373	70.8373
4	126.431	126.431
5	201.122	201.122

Tapered Beam Analysis

In this section, we consider a tapered rotating beam with cantilevered boundary conditions. The same examples were studied by Wright et al.[23] and Hodges and Rutkowski.[2] Banerjee[26] also used them to validated his dynamic stiffness matrix method. For the tapered beams, Banerjee discretized the taper beam using many uniform elements, which results in a stepped beam with piecewise uniform mass and flexural stiffness distribution. Then by assembling these elements, the natural frequencies of a tapered beam can be determined. We included these results to validate our tapered spectral finite element model. In the following two examples, we only use one single spectral finite element to calculate the natural frequencies.

Tapered Beam 1

The mass distribution was assumed to be linear:

$$m(x) = m_0[1 - 0.5(x/L)] \tag{29}$$

The flexural stiffness $EI(x)$ was

$$EI(x) = EI_0[1 - 0.5(x/L)]^3 \tag{30}$$

Taper parameters were

$$\alpha = -0.5, \qquad \beta_1 = 3\alpha = -1.5$$

$$\beta_2 = 3\alpha^2 = 0.75, \qquad \beta_3 = \alpha^3 = -0.125, \qquad \beta_4 = 0$$

As shown in Table 3, we calculated the first three modal frequencies, and the rotating speeds varied from 0 to 12. A single spectral finite element was used in our analysis, and we included first 80 terms in the Frobenius power series. Hodges and Rutkowski[2] used one finite element with 15-order polynomial functions as the interpolation functions. For the three modal frequencies, our predictions

Table 3 Predictions of nondimensional natural frequencies of tapered cantilevered beam[a] under different rotation speeds

	First mode			Second mode			Third mode		
Rotating speed λ	Present SFEM, $NE=1$	Ref. 26 SFEM, $NE=20$	Ref. 2 CFEM, $NE=1$	Present SFEM, $NE=1$	Ref. 26 SFEM, $NE=20$	Ref. 2 CFEM, $NE=1$	Present SFEM, $NE=1$	Ref. 26 SFEM, $NE=20$	Ref. 2 CFEM, $NE=1$
0	3.8238	3.8198	3.8238	18.3173	18.295	18.3173	47.2648	47.203	47.2648
1	3.9866	3.9827	3.9866	18.4740	18.451	18.4740	47.4173	47.356	47.4173
2	4.4368	4.4331	4.4368	18.9366	18.914	18.9366	47.8716	47.810	47.8716
3	5.0927	5.0892	5.0927	19.6839	19.662	19.6839	48.6190	48.558	48.6190
4	5.8788	5.8755	5.8788	20.6852	20.664	20.6852	49.6456	49.586	49.6456
5	6.7434	N/A	6.7345	21.9053	N/A	21.9053	50.9338	N/A	50.9338
6	7.6551	N/A	7.6551	23.3093	N/A	23.3093	52.4633	N/A	52.4633
7	8.5956	N/A	8.5956	24.8647	N/A	24.8647	54.2124	N/A	54.2124
8	9.5540	N/A	9.5540	26.5437	N/A	26.5437	56.1595	N/A	56.1595
9	10.5239	N/A	10.5239	28.3227	N/A	28.3227	58.2833	N/A	58.2833
10	11.5015	N/A	11.5015	30.1827	N/A	30.1827	60.5639	N/A	60.5639
11	12.4845	N/A	12.4845	32.1085	N/A	32.1085	62.9829	N/A	62.9829
12	13.4711	N/A	13.4711	34.0877	N/A	34.0877	65.5237	N/A	65.5237

[a]Parameters: $m(X)=m_0(1-0.5X)$ and $EI(X)=EI_0(1-0.5X)^3$.

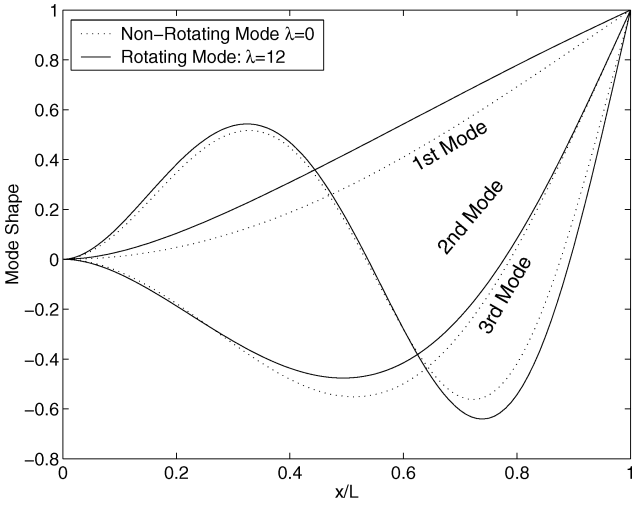

Fig. 4 First three mode shapes of a cantilevered tapered beam: $m(X)=m_0(1-0.5X)$ and $EI(X)=EI_0(1-0.5X)^3$.

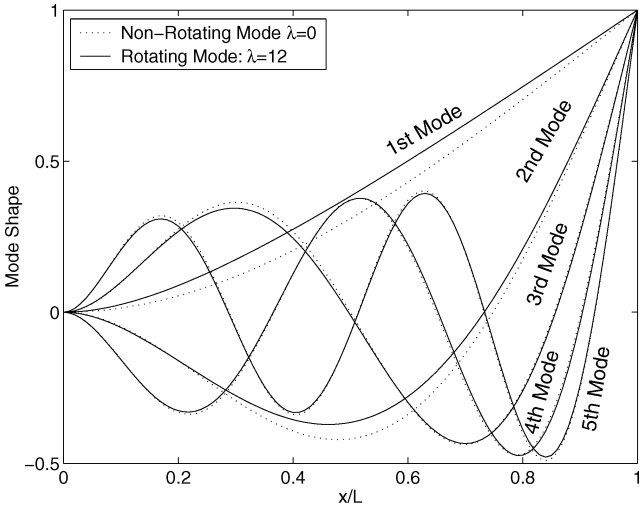

Fig. 5 First five mode shapes of a cantilevered tapered beam: $m(X)=m_0(1-0.8X)$ and $EI(X)=EI_0(1-0.95X)$.

exactly match with the results of Hodges and Rutkowski,[2] where the rotation speed λ varied from 0 to 12. For the lower modes, the CFEM and spectral FEM SFEM yield similar accuracy for the frequency predictions. Banerjee[26] also studied the same example using uniform rotating dynamic stiffness method, where 20 elements were included, and the results were calculated only when $\lambda \leq 4$. The natural frequency predictions degrade compared to our results and those in Ref. 2. From an engineering point of view, the results were sufficient. However, it suggested that, for a tapered beam, the exact displacement solutions were very critical to obtain an accurate dynamic stiffness matrix. Figure 4 shows the first mode shapes for this tapered beam. We plotted both rotating and nonrotating modes. We found that, by increasing the modal number, the discrepancies between the rotating and nonrotating mode shapes become much smaller; however, the natural frequencies were quite different, as shown in Table 3.

Tapered Beam 2

To validate our spectral finite element model further, we considered another tapered beam, which was used by Wright et al.[23] The tapered beam has a linear variation in both mass and flexural stiffness:

$$m(x) = m_0[1 - 0.8(x/L)], \qquad EI(x) = EI_0[1 - 0.95(x/L)]$$

As mentioned by Wright et al.,[23] this beam design was used in windmill turbine blades. As shown in the preceding equation, when $x = L$, the flexural stiffness drops to 5% of initial value of EI_0. The singularity is very closed to $x = L$, which results in the slower convergence of power series. To remedy this problem, Wright et al.[23] expanded the Frobenius functions at $x = 1/0.95$. This implied that we must include more terms in the calculation of Frobenius function without shifting the expansion points in the Frobenius function. We included first 350 terms in the Frobenius functions. However, we still need only one spectral finite element. The taper parameters are defined as

$$\alpha = -0.8, \qquad \beta_1 = -0.95, \qquad \beta_2 = \beta_3 = \beta_4 = 0$$

We validated our natural frequency results for first five modes using the exact solutions by Wright et al.,[23] as shown in Tables 4 and 5, in which the boundary conditions are cantilevered and hinged, respectively. We achieve almost the same accuracy in all natural frequency calculations in both cases with the rotating speed varying from 0 to 12. However, for the fifth mode, our predictions were slightly higher than those by Wright et al.[23] We could improve our frequency prediction by including more terms in the Frobenius functions. However, our spectral finite element model and that of Wright et al. were both based on the exact solutions. Therefore, the differences arises from numerical errors. Again, these two analyses provides equivalently accurate results from an engineering perspective. Figure 5 and 6 show the first five mode shapes for cantilevered and hinged beams, respectively. Both rotating, $\lambda = 12$, and nonrotating mode shapes are shown. The effect of rotation on the rotating beam mode shape was

Table 4 Predictions of nondimensional natural frequencies of tapered cantilevered beam[a] under different rotation speeds

Rotating speed λ	First mode		Second mode		Third mode		Fourth mode		Fifth mode	
	Present	Ref. 23	Present	Ref. 23	Present	Ref. 23	Present	Ref. 23	Present	Ref. 23
0	5.2738	5.2738	24.0041	24.0041	59.9708	59.9708	112.892	112.909	183.473	183.024
1	5.3903	5.3903	24.1069	24.1069	60.0703	60.0696	112.992	113.009	183.576	183.124
2	5.7249	5.7249	24.4129	24.4130	60.3676	60.3669	113.290	113.307	183.887	183.424
3	6.2402	6.2402	24.9148	24.9149	60.8598	60.8590	113.784	113.803	184.404	183.923
4	6.8928	6.8928	25.6013	25.6013	61.5420	61.5412	114.472	114.492	185.127	184.619
5	7.6443	7.6443	26.4580	26.4581	62.4078	62.4069	115.351	115.372	186.055	185.509
6	8.4653	8.4653	27.4692	27.4693	63.4494	63.4483	116.414	116.439	187.186	186.591
7	9.3347	9.3347	28.6184	28.8894	64.6579	64.6566	117.658	117.685	188.520	187.862
8	10.2379	10.2379	29.8893	29.8894	66.0238	66.0222	119.075	119.107	190.055	189.316
9	11.1651	11.1650	31.2667	31.2669	67.5370	67.5351	120.659	120.696	191.793	190.950
10	12.1092	12.0192	32.7367	32.7369	69.1875	69.1851	122.403	122.446	193.734	192.759
11	13.0657	13.0657	34.2868	34.2871	70.9653	70.9622	124.298	124.350	195.882	194.737
12	14.0313	14.0313	35.9060	35.9064	72.8604	72.8565	126.336	126.401	198.243	196.880

[a]Parameters: $m(X) = m_0(1 - 0.8X)$ and $EI(X) = EI_0(1 - 0.95X)$.

Table 5 Predictions of nondimensional natural frequencies of tapered hinged beam[a] under different rotation speeds

Rotating speed λ	First mode		Second mode		Third mode		Fourth mode		Fifth mode	
	Present	Ref. 23	Present	Ref. 23	Present	Ref. 23	Present	Ref. 23	Present	Ref. 23
0	0.0000	0.0000	16.7328	16.7328	48.4696	48.4691	97.1599	97.1704	163.277	163.002
1	1.0000	1.0000	16.8711	16.8711	48.5876	48.5872	97.2717	97.2823	163.388	163.111
2	2.0000	2.0000	17.2793	17.2794	48.9399	49.9395	97.6062	97.6172	163.723	163.438
3	3.0000	3.0000	17.9389	17.9388	49.5214	49.5210	98.1611	98.1727	164.281	163.983
4	4.0000	4.0000	18.8233	18.8233	50.3239	50.3234	98.9324	98.9450	165.059	164.741
5	5.0000	5.0000	19.9022	19.9022	51.3366	51.3360	99.9147	99.9287	166.055	165.771
6	6.0000	6.0000	21.1456	21.1456	52.5471	52.5463	101.102	101.117	167.268	166.889
7	7.0000	7.0000	22.5259	22.5260	53.9415	54.9405	102.485	102.504	168.695	168.269
8	8.0000	8.0000	24.0194	24.0195	55.5054	55.5042	104.058	104.079	170.333	169.847
9	9.0000	9.0000	25.6059	25.6060	57.2245	57.2230	105.809	105.835	172.180	171.618
10	10.0000	10.0000	27.2690	27.2692	59.0847	59.0828	107.730	107.762	174.236	173.573
11	11.0000	11.0000	28.9953	28.9956	61.0727	61.0700	109.810	109.850	176.500	175.708
12	12.0000	12.0000	30.7741	30.7745	63.1758	63.1722	112.040	112.090	178.978	178.105

[a]Parameters $m(X) = m_0(1 - 0.8X)$ and $EI(X) = EI_0(1 - 0.95X)$.

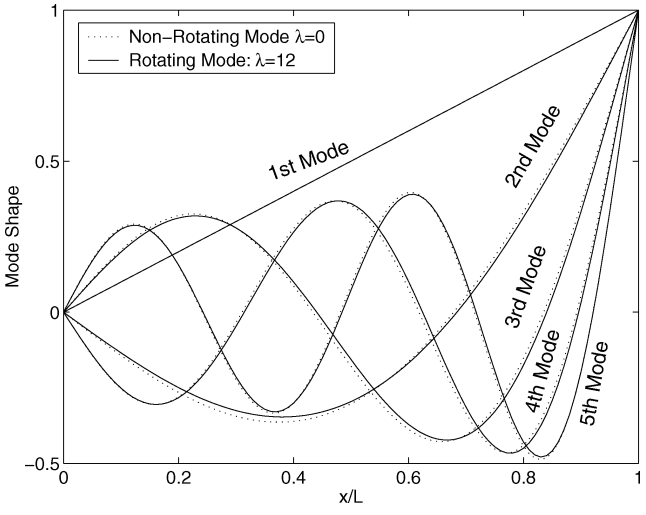

Fig. 6 First five mode shapes of a hinged tapered beam: $m(X) = m_0(1-0.8X)$ and $EI(X) = EI_0(1-0.95X)$.

substantially diminished for mode number greater than 3, so that the rotating and nonrotating mode shapes became similar. However, the natural frequency results were significantly different in both cases.

Tapered SFEM vs Uniform SFEM

Bannerjee[26] also validated his results using the preceding example, in which cantilevered boundary conditions were assumed. He approximated the linearly tapered beam using many uniform beam elements. His uniform spectral finite element model can then be applied to solve the tapered beam case. Because we developed a tapered spectral finite element model for rotating beams directly, we need one single element in our analysis. There is no need to approximate a tapered beam using uniform elements. As discussed by Banerjee,[26] the effects of hub offset length $\bar{R}$ on the natural frequency predictions were studied. Table 6 compares our tapered spectral finite element results to Banerjee's predictions, in which the hub offset length $\bar{R}$ varied from 1 to 5 and rotating speed is either 1 or 5. There are a total of four possible combinations, as shown in Table 6. Banerjee[26] used 20 and 50 elements in his calculations. We found that the natural frequency predictions based on 50 elements were superior and correlated with our results, in which only one tapered spectral finite element was used.

Nonuniform Beam Analysis

Hodges[13] developed a direct Ritz method for nonuniform rotating beams with discontinuities in bending stiffness and mass distribution. The nondimensional mass and stiffness distributions were $x = 0.05 \le x/L \le 0.2$, $m(x)/m_0 = 1$, and $EI(x)/EI_0 = 0.00146$ and $x = 0.2 \le x/L \le 1$, $m(x)/m_0 = 5[1 - 0.5(x/L)]$, and $EI(x)/EI_0 = 0.0146[1 - (3/2)(x/L) + (3/4)(x^2/L^2)]$.

The hub offset length was $\bar{R} = 0.05$, and nondimensional rotating speed is $\lambda = 1$. It was a hingeless rotor, and cantilevered boundary conditions were assumed. Hodges[13] used a total of five elements to obtain a convergent natural frequency calculation up to the fourth bending vibration mode, in which polynomial admissible functions with order to 10 were assumed in each element. In our spectral finite element model, because there are two taper changes in the rotor system, we only need to include two tapered elements to account for the discontinuities of mass and stiffness distribution. We included

Table 6 Predictions of nondimensional natural frequencies of tapered cantilevered beam[a]

Mode	Present, $NE=1$	Banerjee[26,b] $NE=50$	Banerjee[26,b] $NE=20$
	$\lambda=1,\ \bar{R}=1$		
1	5.5506	5.5493	5.5427
2	24.250	24.241	24.195
3	60.214	60.186	60.043
	$\lambda=5,\ \bar{R}=1$		
1	10.083	10.082	10.076
2	29.534	29.525	29.484
3	65.765	65.737	65.599
	$\lambda=1,\ \bar{R}=5$		
1	6.1494	6.1482	6.1418
2	24.813	24.804	24.759
3	60.786	60.758	60.615
	$\lambda=5,\ \bar{R}=5$		
1	16.512	16.51	16.504
2	39.411	39.404	39.362
3	77.610	77.575	77.439

[a]Variations of rotation speeds, hub offset length $\bar{R}\neq 0$, $m(X)=m_0(1-0.8X)$, and $EI(X)=EI_0(1-0.95X)$.
[b]Uniform beam SFEM used.

Table 7 Nondimensional natural frequencies of cantilevered nonuniform beam with discontinuities in mass and stiffness distribution[a]

Mode	Present SFEM, $N=2$	Hodges[13] CFEM, $N=5$
1	1.0660075	1.0660084
2	2.5906956	2.5906956
3	4.7187589	4.7187589
4	7.6691747	7.6691747

[a]Rotation speed $\lambda=1$, and hub offset $\bar{R}=0.05$.

200 terms in the Frobenius series. Table 7 shows the first four natural frequency results. The analyses agree with each other. However, only two elements are required in our spectral finite element analysis to achieve comparable accuracy compared to Hodges's results using five elements.

Conclusions

We have validated our spectral finite element results for uniform beams and beams with single taper or compound taper under multiple rotating speeds. Both cantilevered and hinged boundary conditions were considered. It has been shown that our spectral finite element model can provide comparable or better accuracy for the natural frequency predictions. The natural frequency predictions can achieve up to six digit accuracy compared to those results in the literature. Because our spectral finite element model was based on the exact wave propagation solutions, only a single element is sufficient to capture the complete dynamic characteristics of a rotating beam, as long as the beam impedance does not change. The minimum number of such spectral finite element coincides with the number of substructures in a blade system.

When the spectral finite element model is used, the calculation of natural frequency in the beam free vibration is executed by solving a transcendental equation. The process is straightforward and can be easily realized by many optimization software codes, such as MATLAB software.

Therefore, our spectral finite element model can be used in the dynamic analysis of rotating uniform or tapered beams with substantially reduced degrees of freedom having higher accuracy. The same methodologies of SFEM can be extended to coupling motions of rotating tapered blades, where flap, lag, and torsion motions were fully coupled.

References

[1]Leissa, A., "Vibration Aspects of Rotating Turbomachinery Blades," *Applied Mechanics Review*, Vol. 34, No. 5, 1981, pp. 629–635.

[2]Hodges, D. H., and Rutkowski, M. J., "Free Vibration Analysis of Rotating Beams by a Variable-Order Finite Element Method," *AIAA Journal*, Vol. 19, No. 11, 1981, pp. 1459–1466.

[3]Boyce, W. E., "Effect of Hub Radius on the Vibration of Uniform Bar," *Journal of Applied Mechanics*, Vol. 23, No. 2, 1956, pp. 287–290.

[4]Hunter, W. F., "Integrating Matrix Method for Determining the Natural Vibration Characteristics of Propeller Blades," NASA TN D-6064, Dec. 1970.

[5]Pnueli, D., "Natural Bending Frequency Comparable to Rotational Frequency in Rotating Cantilever Beam," *Journal of Applied Mechanics*, Vol. 39, No. 2, 1972, pp. 602–604.

[6]Lo, H., Goldberg, J. E., and Bogdanoff, J. L., "Effect of Small Hub-Radius Change on Bending Frequencies of a Rotating Beam," *Journal of Applied Mechanics*, Vol. 27, No. 4, 1960, pp. 548–550.

[7]Peters, D. A., "An Approximate Solutions for the Free Vibrations of Rotating Uniform Cantilever Beams," NASA TM X-62,299, Sept. 1973.

[8]Nagaraj, V. T., and Shanthakumar, P., "Rotor Blade Vibrations by the Galerkin Finite Element Method," *Journal of Sound and Vibration*, Vol. 43, No. 3, 1975, pp. 575–577.

[9]Murty, A. V. K., and Murthy, S. S., "Finite Element Analysis of Rotors," *Mechanism and Machine Theory*, Vol. 12, No. 4, 1977, pp. 311–322.

[10]Dzygadlo, Z., and Sobieraj, W., "Natural, Flexural–Torsional Vibration Analysis of Helicopter Rotor Blades by the Finite Element Method," *Journal of Technical Physics*, Vol. 18, No. 4, 1977, pp. 443–454.

[11]Putter, S., and Manor, H., "Natural Frequencies of Radial Rotating Beams," *Journal of Sound and Vibration*, Vol. 56, No. 2, 1978, pp. 175–185.

[12]Hoa, S. V., "Vibration of a Rotating Beam with Tip Mass," *Journal of Sound and Vibration*, Vol. 67, No. 3, 1979, pp. 369–381.

[13]Hodges, D. H., "Vibration of Response of Nonuniform Rotating Beams with Discontinuities," *Journal of the American Helicopter Society*, Vol. 24, No. 5, 1979, pp. 43–50.

[14]Khulief, Y. A., "Vibration Frequencies of a Rotating Tapered Beam with End Mass," *Journal of Sound and Vibration*, Vol. 134, No. 1, 1989, pp. 87–97.

[15]Udupa, K. M., and Varadan, T. K., "Hierarchical Finite Element Method for Rotating Beams," *Journal of Sound and Vibration*, Vol. 138, No. 3, 1990, pp. 447–456.

[16]Washizu, K., *Variational Methods in Elasticity and Plasticity*, Pergamon, Oxford, 1968.

[17]Doyle, J. F., *Wave Propagation in Structures*, 2nd ed., Springer-Verlag, Berlin, 1997, Chap. 5.

[18]Leung, A. Y. T., *Dynamic Stiffness and Substructures*, Springer-Verlag, London, 1993, Chap. 2.

[19]Wang, G., and Wereley, N. M., "Spectral Finite Element Analysis of Sandwich Beams with Passive Constrained Layer Damping," *Journal of Vibration and Acoustics*, Vol. 124, No. 3, 2002, pp. 376–386.

[20]Ince, E. L., *Ordinary Differential Equations*, Dover, New York, 1956, Chap. 14.

[21]Arfken, G. B., and Weber, H. J., *Mathematical Methods for Physicists*, Academic Press, San Diego, CA, 1995, Chap. 8.

[22]Giurgiutiu, V., and Stafford, R. Q., "Semi Analytical Methods for Frequencies and Mode Shapes of Rotor Blades," *Vertica*, Vol. 1, No. 4, 1977, pp. 291–306.

[23]Wright, A. D., Smith, C. E., Thresher, R. W., and Wang, J. L. C., "Vibration Modes of Centrifugally Stiffened Beams," *Journal of Applied Mechanics*, Vol. 49, No. 2, 1982, pp. 197–202.

[24]Harris, F. D., "The Rotor Blade Flap Bending Problem—An Analytical Test Case," *Journal of the American Helicopter Society*, Vol. 37, No. 4, 1992, pp. 64–67.

[25]Naguleswaran, S., "Lateral Vibration of a Centrifugally Tensioned Uniform Euler–Bernoulli Beam," *Journal of Sound and Vibration*, Vol. 176, No. 5, 1994, pp. 613–624.

[26]Banerjee, J. R., "Free Vibration of Centrifugally Stiffened Uniform and Tapered Beams Using the Dynamic Stiffness Method," *Journal of Sound and Vibration*, Vol. 233, No. 5, 2000, pp. 857–875.

[27]Huang, K. J., and Liu, T. S., "Dynamic Analysis of Rotating Beams with Nonuniform Cross Sections Using the Dynamic Stiffness Method," *Journal of Vibration and Acoustics*, Vol. 123, No. 4, 2001, pp. 536–539.

[28]Johnson, W., *Helicopter Theory*, Dover, New York, 1980, Chap. 9.

[29]Inman, D. J., *Engineering Vibration*, Prentice-Hall, Englewood Cliffs, NJ, 1994, Chap. 6.

A. Berman
Associate Editor